Supplementary information

Phenylboronic acid modification augments the lysosome escape and antitumor efficacy of a cylindrical polymer brush-based prodrug

Ruonan Wang, Changfeng Yin, Changren Liu, Ying Sun, Panpan Xiao, Jia Li, Shuo Yang, Wei Wu, and Xiqun Jiang*

Department of Polymer Science & Engineering, College of Chemistry & Chemical Engineering, Nanjing University, Nanjing 210023, P. R. China

* To whom correspondence should be addressed.

E-mail: wuwei@nju.edu.cn

Table of Contents

Materials and characterizations

Materials

2,2-azodiisobutylnitrile (AIBN), glycidyl methacrylate (GMA), cuprous bromide (CuBr), *N*,*N*,*N*′,*N*′,*N*″-pentamethyldiethylenetriamine (PMDETA), 2-(dimethylamino) ethyl methacrylate (DMAEMA), propargyl bromide, pentynoic acid, *tert*-butyl carbazate, *tert*-butyl bromoacetate, trifluoroacetic acid (TFA) were obtained from J&K Scientific Ltd. Poly(ethylene glycol) monomethyl ether methacrylate (PEGMA, Mn = 350 g mol^{-1}), sodium azide, 2-bromoisobutyryl bromide, NIR-797-isothiocyanate, 4-carboxyphenylboronic acid pinacol ester, fluorescein Isothiocyanate (FITC), and rhodamine B 5-isothiocyanate (RBITC), poly(2-hydroxyethyl methacrylate) (poly-HEMA)were purchased from Sigma-Aldrich. GMA and PEGMA were passed through a basic alumina column to remove the inhibitor before used. CT26, MCF-7, HepG2 and H22 cells were purchased from Shanghai Institute of Cell Biology (Shanghai, China).

Characterizations

^{1}H NMR spectroscopy was recorded on a Bruker AVANCE III 400 and a Bruker AVANCE III HD 500 spectrometer with tetramethylsilane as internal standard. CLSM observations were conducted on LSM-710 (Zeiss Inc., Germany). Gel permeation chromatography (GPC) results were measured by Polymer Laboratories PL-GPC 50 instrument with DMF (0.01 M LiBr) or H_2O (0.2 M $NaNO_3$, 0.2 M Guanidine Hydrochloride, 50% MeOH) as the eluent. Atomic force microscopy (AFM) images were taken on a Bruker ICON Atomic Force Microscope in tapping mode in air at room temperature with OLTESPA-R3 silicon tip (k = 2 N/m, f_0= 70 kHz). The samples were

prepared by drop-cast onto freshly cleaved mica from 0.005 mg/mL aqueous solution. The flow cytometry data were recorded on a Beckman CytoFlex.

In vitro cytotoxicity

MTT assay was used to test the cytotoxicity of BCPB-B-DOX and BCPB-DOX against CT26, MCF-7, and HepG2 cells. Blank polymer brushes and free DOX were set as negative and positive control, respectively. Tumor cells (5×10^3 per well) were seeded in a 96 well plate at 37℃. After growing for 24 h, the cells were treated with blank polymer brushes, free DOX and DOX-loaded polymer brushes at a series of doses for another 24 h. After removal of the culture medium, the cells were washed with PBS three times and cultured in the medium containing MTT for 4 h. Then the medium was removed and 100 μL of DMSO was added to dissolve the produced formazan. The absorbance of formazan at 570 nm was measured by a microplate reader (Safire, Tecan).

Cellular uptakes

The cellular uptake behaviors of BCPB-B-DOX and BCPB-DOX were studied in CT26, MCF-7, and HepG2 cells. Tumor cells (1×10^5 per well) were seeded in a 6 well plate, and incubated at 37℃ for 24 h, and then treated with the FITC-labeled BCPB-B-DOX and BCPB-DOX at a dose of 5 μg/mL DOX equivalent, respectively. After 4 h coincubation, the cells were imaged by CLSM.

Lysosome escape

The lysosome escape behaviors of BCPB-B and BCPB were studied in CT26, MCF-7, and HepG2 cells. The tumor cells (1×10^5 per well) were seeded in a 6 well plate and incubated at 37 ℃ for 24 h. Thereafter, the FITC-labeled BCPB-B and BCPB were

added and incubated at 37 ℃ for predetermined periods. The lysosome was labeled with LysoTracker red before CLSM observations. For the GeneOntology (GO) pathway analysis, alkynyl-bearing Fe_3O_4 nanoparticles (the diameter is ~10 nm) were conjugated to BCPB-B-N_3 and BCPB-N_3 via CuAAC, respectively. Then the Fe_3O_4-modified BCPB-B and BCPB were incubated with the cells at 37 ℃ for 12 h, respectively. After washed with PBS 3 times, the cells were lysed by using RIPA Lysis Buffer. The Fe_3O_4-modified BCPB-B and BCPB together with the adsorbed proteins were collected via magnetic separation, respectively. After washing out the non-specifically adsorbed proteins from the Fe_3O_4-modified CPBs, we collected the specifically adsorbed proteins by extraction with loading buffer at 100 ℃ for 10 min. The specifically adsorbed proteins were determined by nano liquid chromatography-tandem mass spectrometry after in-gel digestion with trypsin.

Penetration in multicellular spheroids (MCs)

The CT26 and HepG2 MCs were prepared in culture flasks coated with poly(2-hydroxyethyl methacrylate)[1]. After growing for 2 weeks, the diameter of the MCs reached 200-300 μm. Certain amount of fluorescence labeled BCPB-B and BCPB were added for coincubation at 37℃ for 6, 12 and 24 h, respectively. The penetration behaviors were visualized via CLSM.

Near-infrared fluorescence (NIRF) imaging

BCPB-B-DOX and BCPB-DOX was labeled with NIR-797-isothiocyanate for realtime NIRF imaging. All the animal experiments were approved and in accordance with the guidelines set by the Institutional Animal Care and Use Committee (IACUC) of

Nanjing University. H22 tumor models were established by injecting subcutaneously 5 $\times 10^5$ H22 cells in 100 μL of saline under the armpit of ICR male mice. After a week, the average volume of H22 tumors reached about 500 mm^3. NIR-797-labeled BCPB-B-DOX and BCPB-DOX were injected by tail vein into tumor-bearing mice, respectively. Then the mice was anesthetized and visualized on the Maestro™ EX fluorescence imaging system (CRi, USA). intravenous (i.v.) injected into H22 tumor-bearing mice via a tail vein

Biodistribution and tumor penetration

H22 tumor models were established in ICR mice with an average volume of about 500 mm^3 for biodistribution quantitative analysis. DOX-loaded polymer brushes were injected into the tumor-bearing mice at a dose of 4 mg kg^{-1} DOX equivalent via tail vein. Tumors, main organs (heart, liver, spleen, lung, kidney) and blood were harvested at different time points after the injection. The blood samples were centrifuged to obtain the serum, and the samples of tumors and normal organs were homogenized. After the extraction via 70% ethanol with 0.3 M HCl for 48 h, the concentrations of DOX were measured by fluorescence spectroscopy at an excitation wavelength of 480 nm and emission wavelength of 590 nm based on a pre-established calibration curve.

In vivo antitumor

H22 tumor model was established in ICR mice with an average volume of about 200 mm^3 for anticancer experiments. Free DOX, BCPB-DOX and BCPB-B-DOX were injected into tumor-bearing mice at a dose of 4 mg kg^{-1} DOX equivalent via tail vein, respectively, with the mice treated by blank polymer brushes and saline as negative

control groups. Each group consisted of 8 mice. Tumor volume (V, $V = a \times b^2/2$, a is the longest diameter and b is the shortest diameter) and body weight were measured every other day, and the survival rate were monitored throughout 60 days. The tumor growth inhibition (TGI) was calculated by the following equation.

$$TGI = 1 - \frac{volume\ \ of\ \ experimental\ \ group}{volume\ \ of\ \ control\ \ group} \times 100\%$$

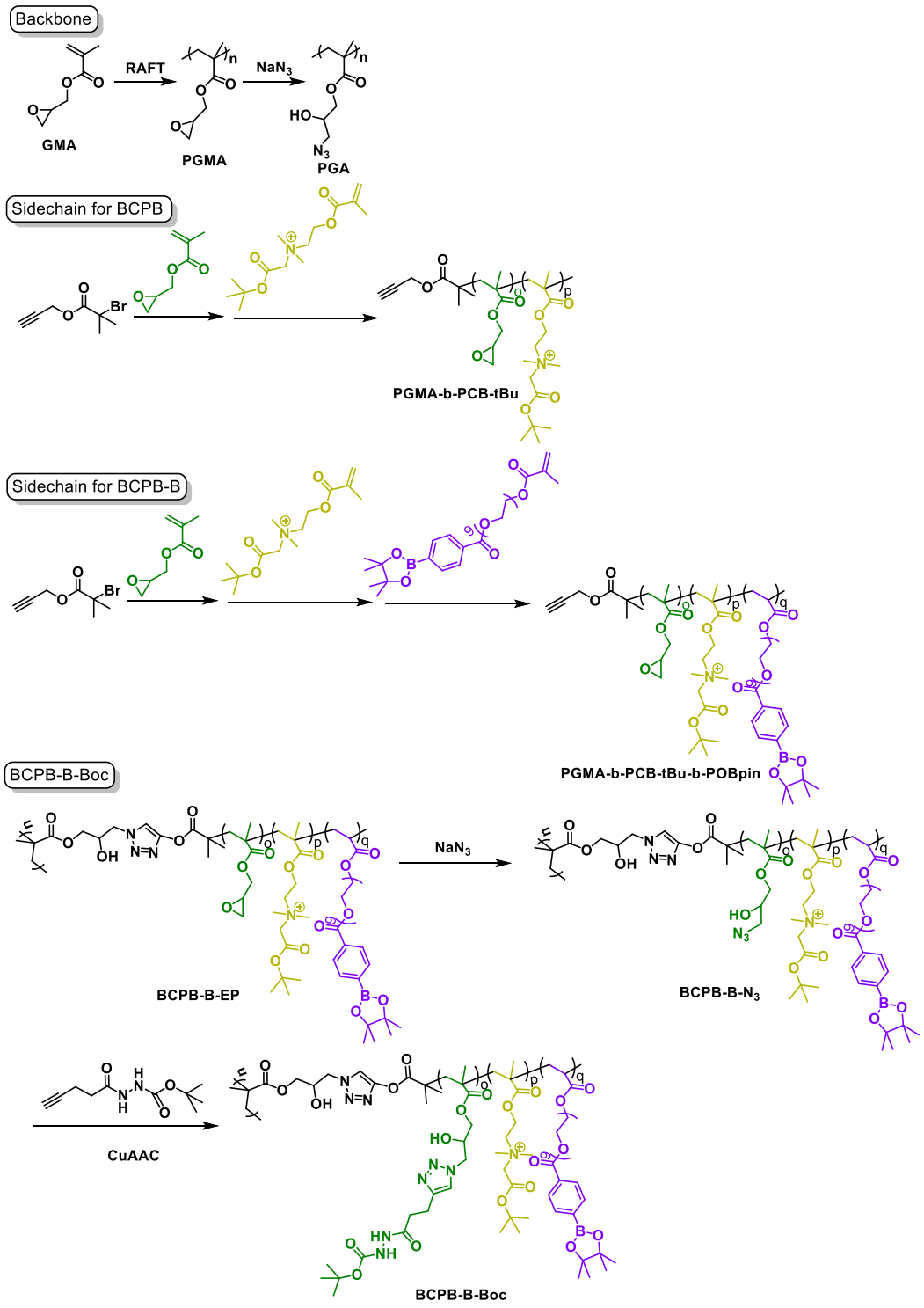

Supplementary Scheme 1. Synthesis routes of the backbone and side chains of the CPBs, and BCPB-B-Boc.

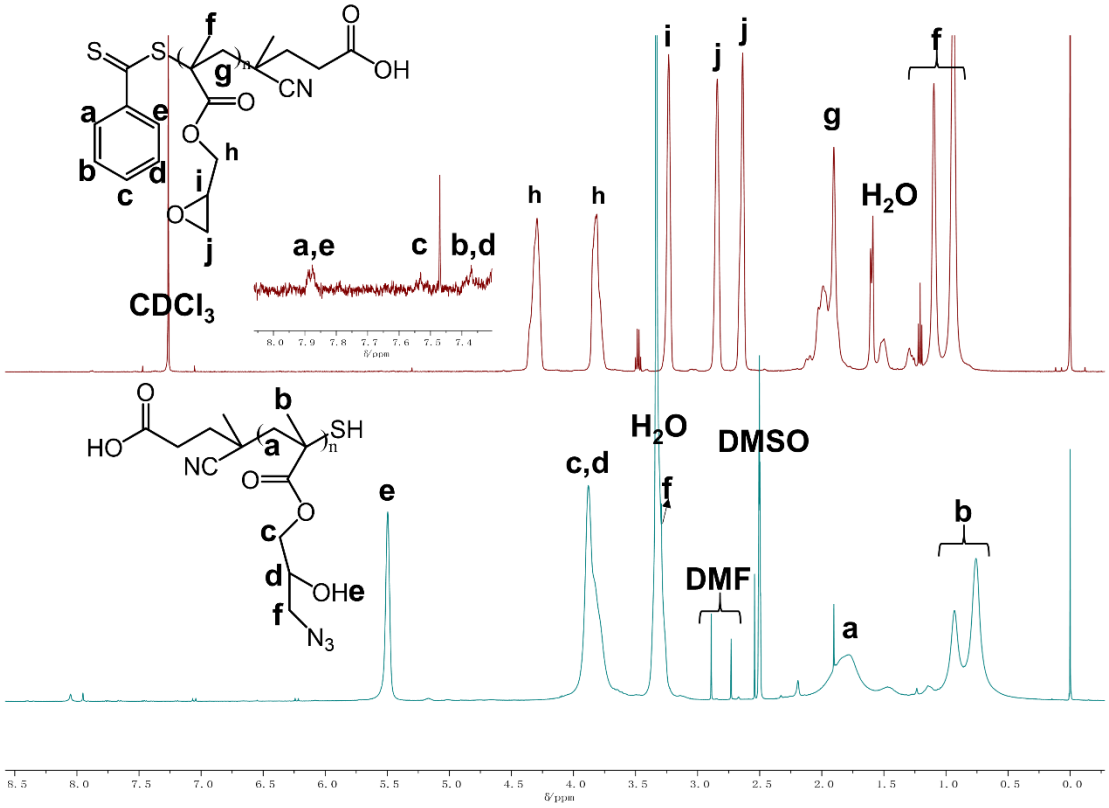

Supplementary Figure 1 ^{1}H NMR spectra of the backbone PGMA (in $CDCl_3$) and PGA (in DMSO-d_6).

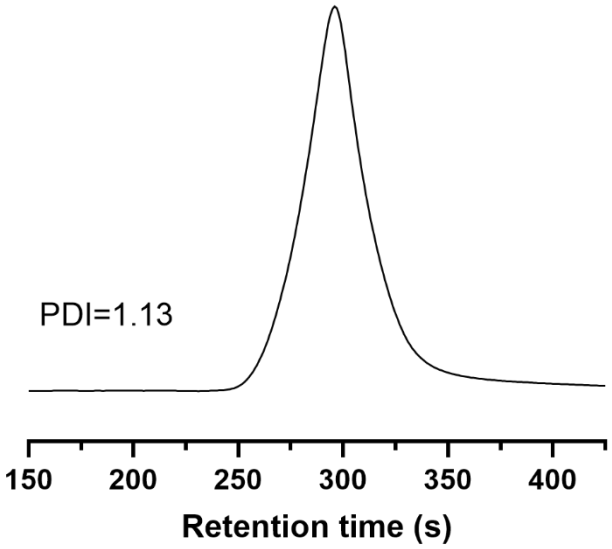

Supplementary Figure 2. GPC curve of the backbone PGMA.

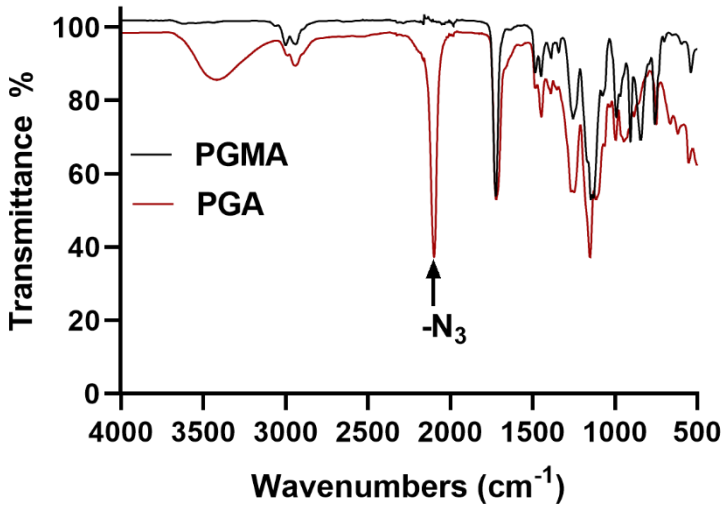

Supplementary Figure 3. FTIR spectra of the backbone PGMA and PGA.

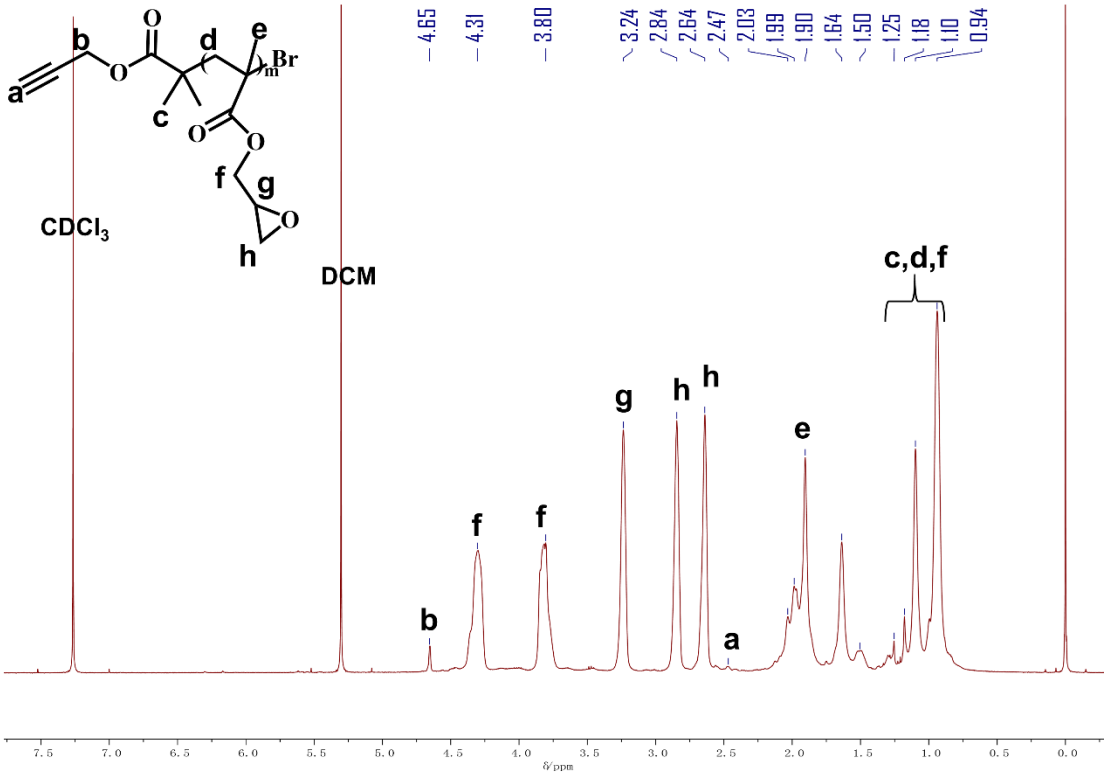

Supplementary Figure 4. ^{1}H NMR spectrum of the side chain PGMA in $CDCl_3$.

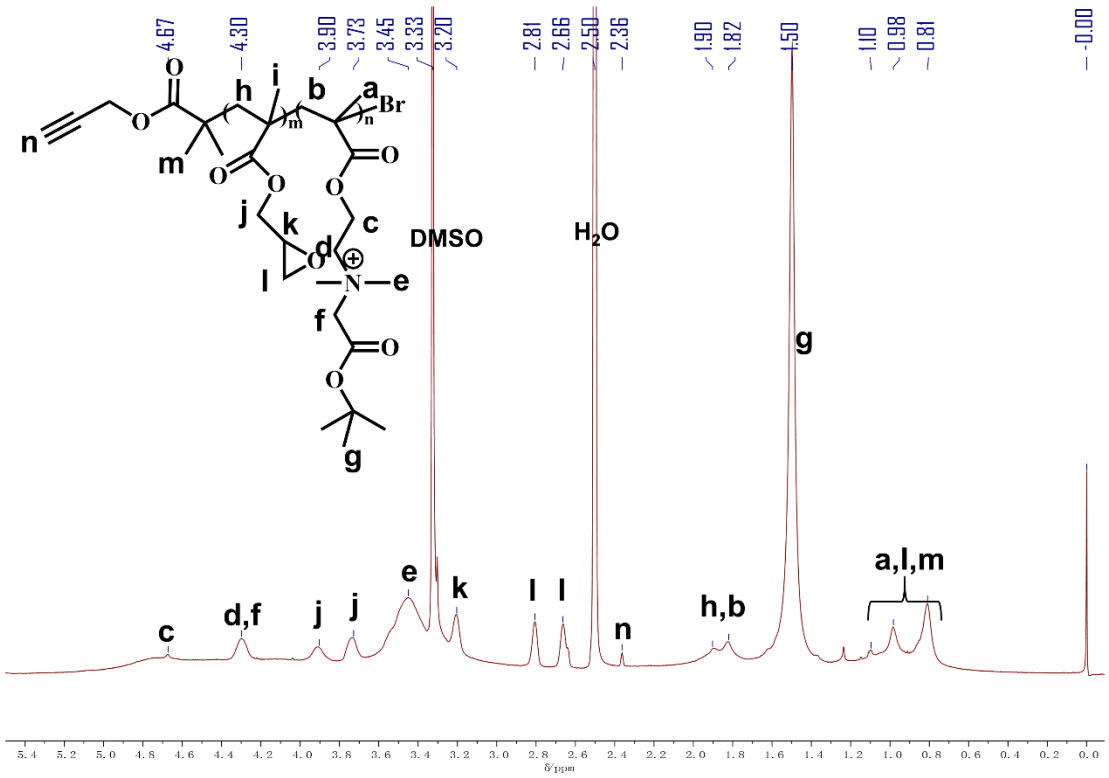

Supplementary Figure 5. ^{1}H NMR spectrum of PGMA-PCB-tBu in DMSO-d_6.

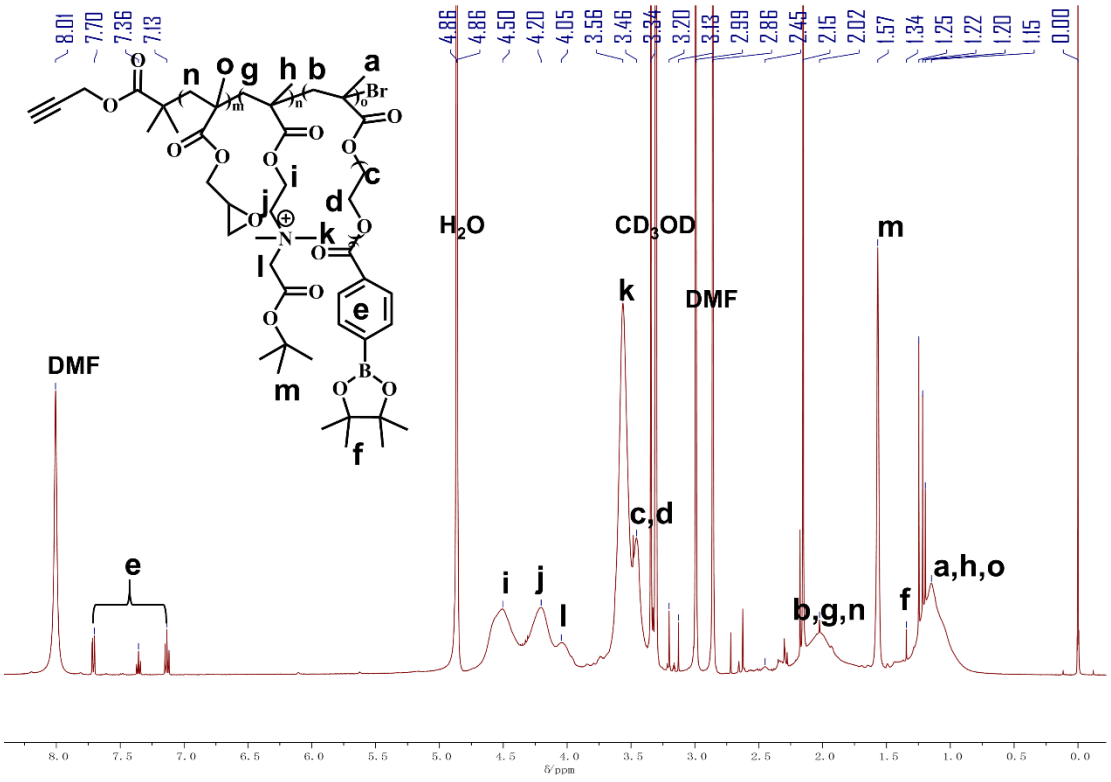

Supplementary Figure 6. ^{1}H NMR spectrum of PGMA-PCB-tBu-POBpin in CD_3OD.

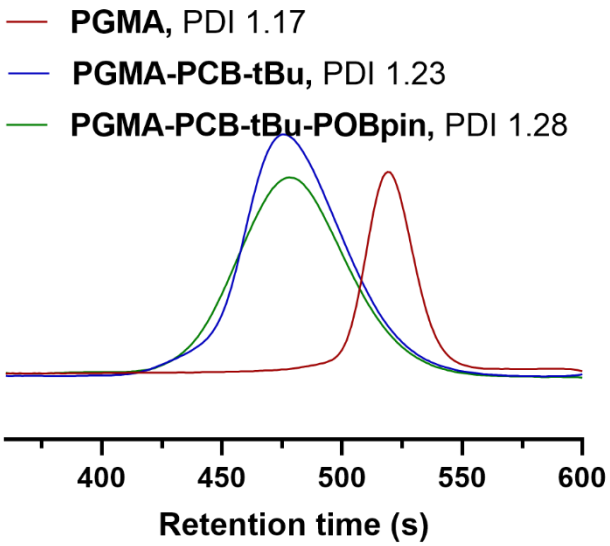

Supplementary Figure 7. GPC curves of PGMA, PGMA-PCB-tBu, and PGMA-PCB-tBu-POBpin.

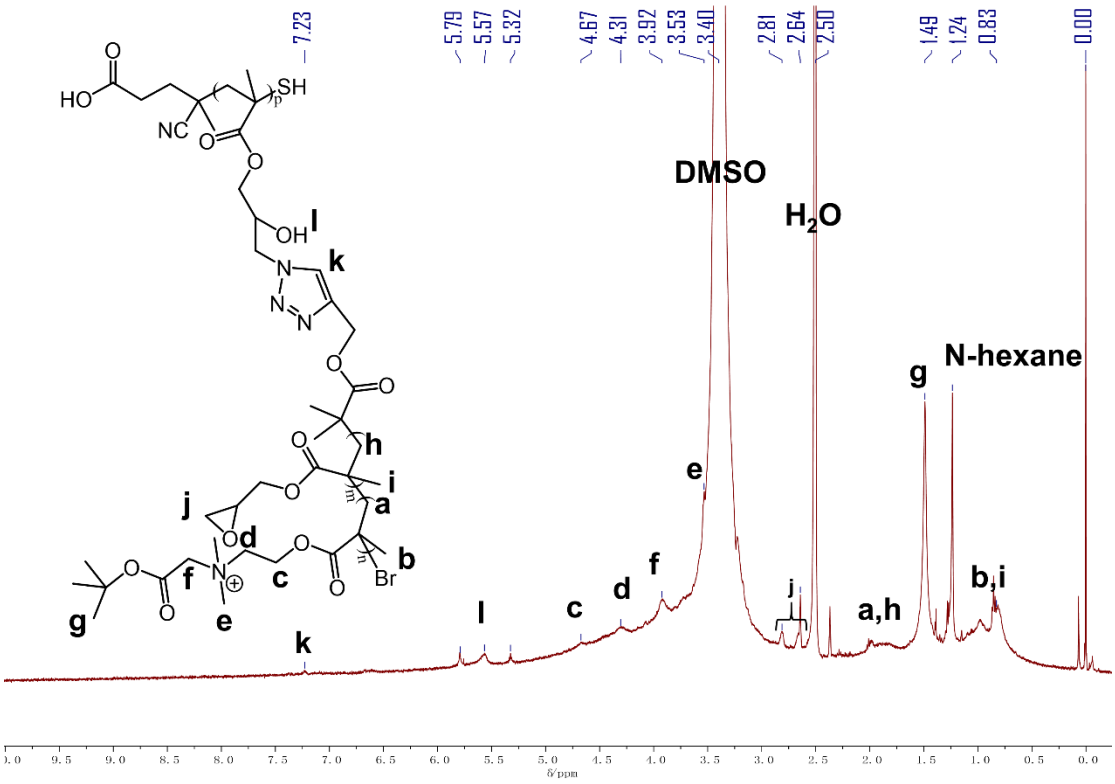

Supplementary Figure 8. ^{1}H NMR spectrum of BCPB-EP in DMSO-d_6.

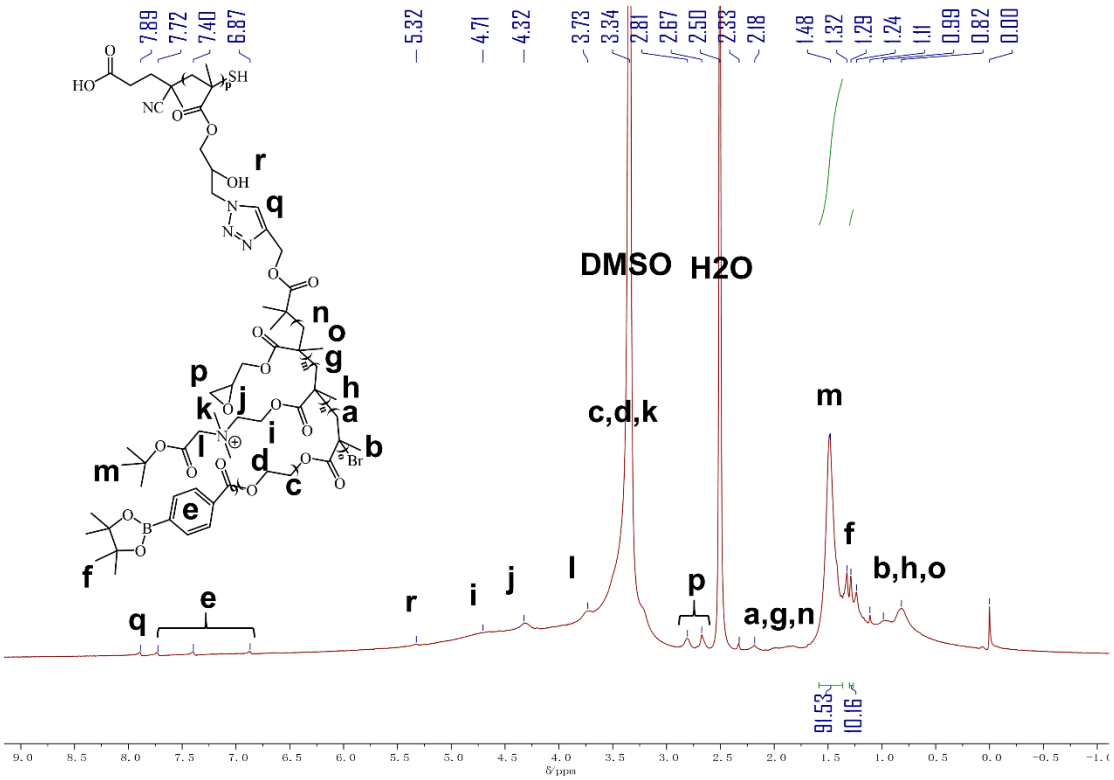

Supplementary Figure 9. ^{1}H NMR spectrum of BCPB-B-EP in DMSO-d_6.

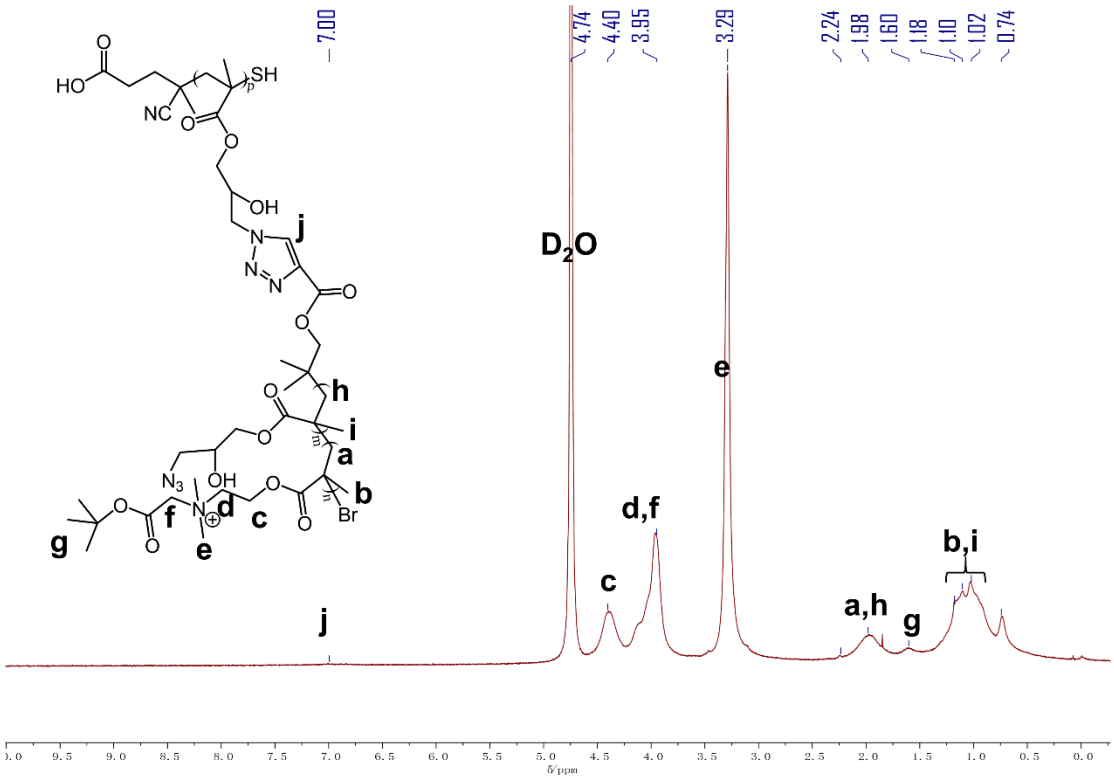

Supplementary Figure 10. ^{1}H NMR spectrum of BCPB-N_3 in D_2O.

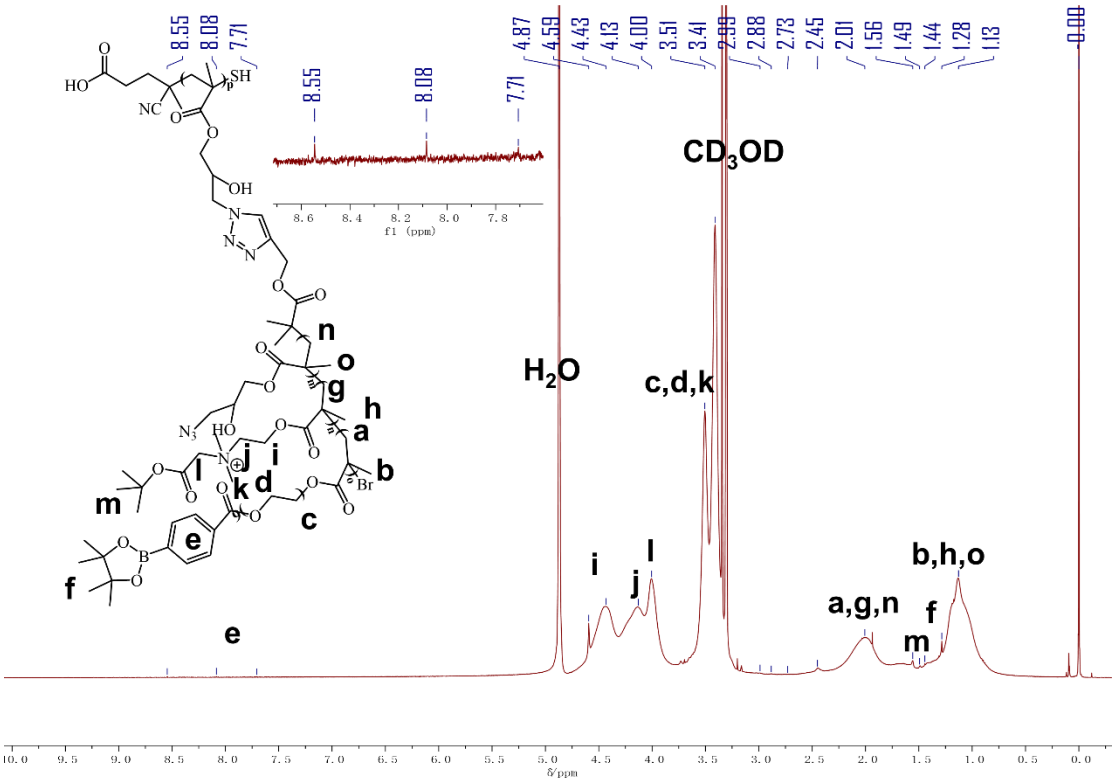

Supplementary Figure 11. ^{1}H NMR spectrum of BCPB-B-N_3 in CD_2OD.

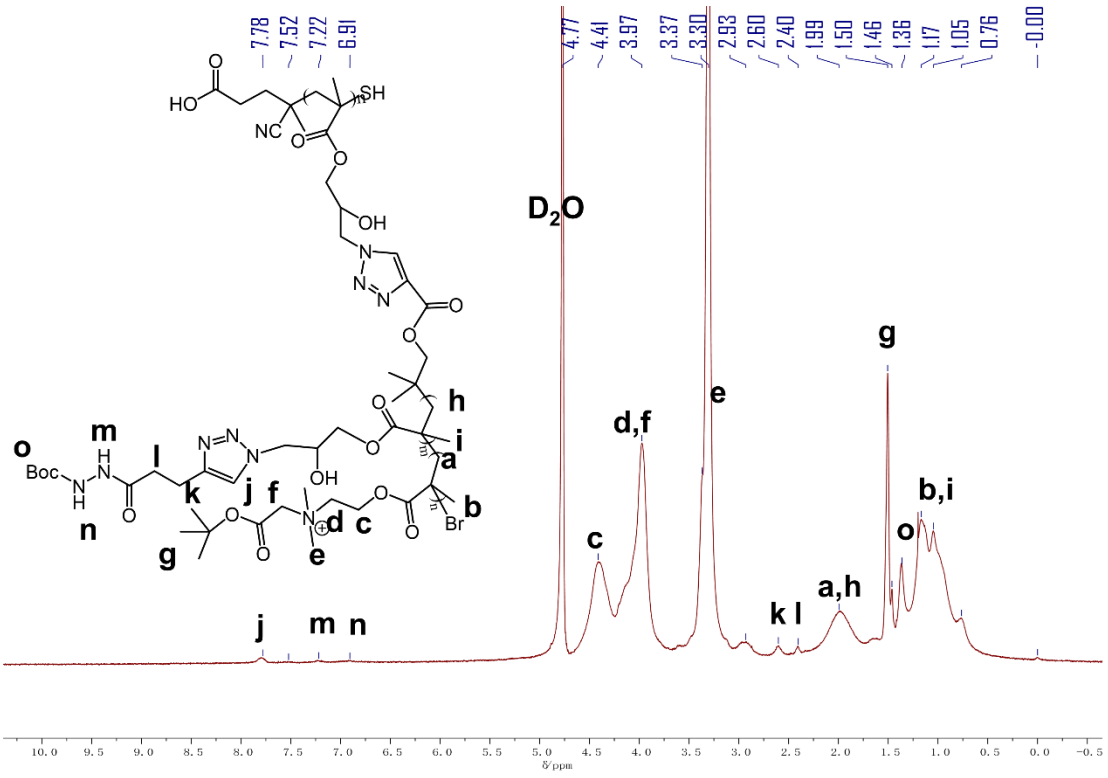

Supplementary Figure 12. ^{1}H NMR spectrum of BCPB-Boc in D_2O.

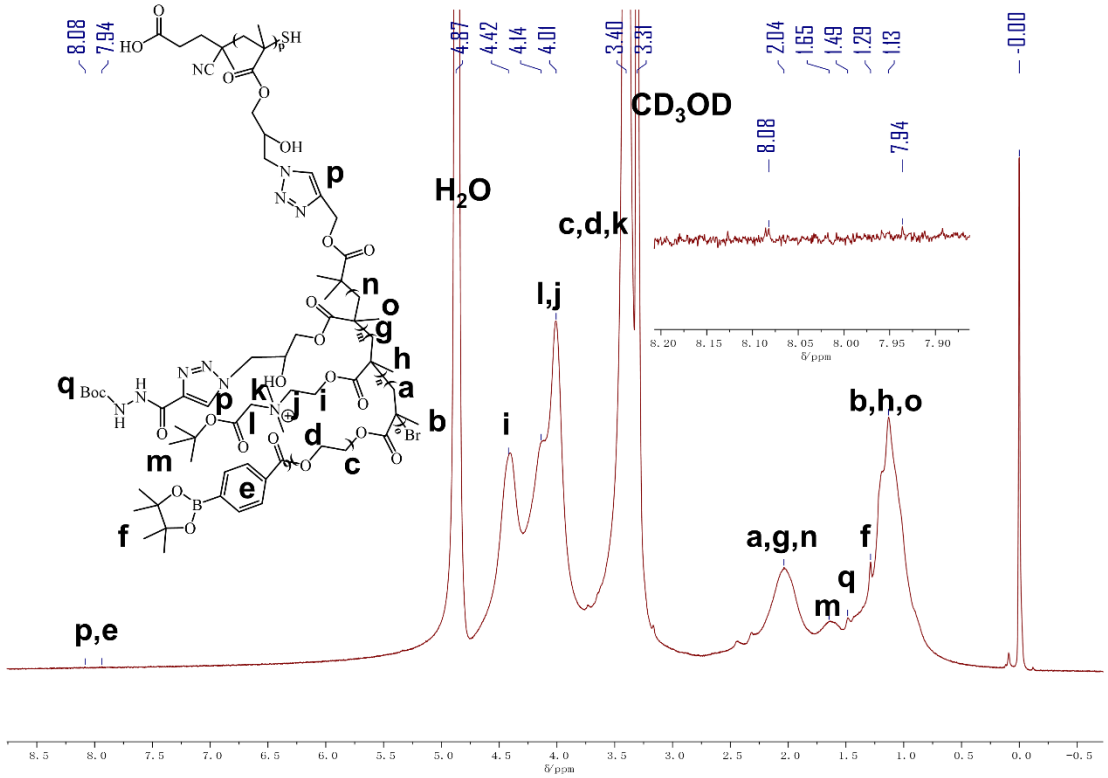

Supplementary Figure 13. ^{1}H NMR spectrum of BCPB-B-Boc in CD_3OD.

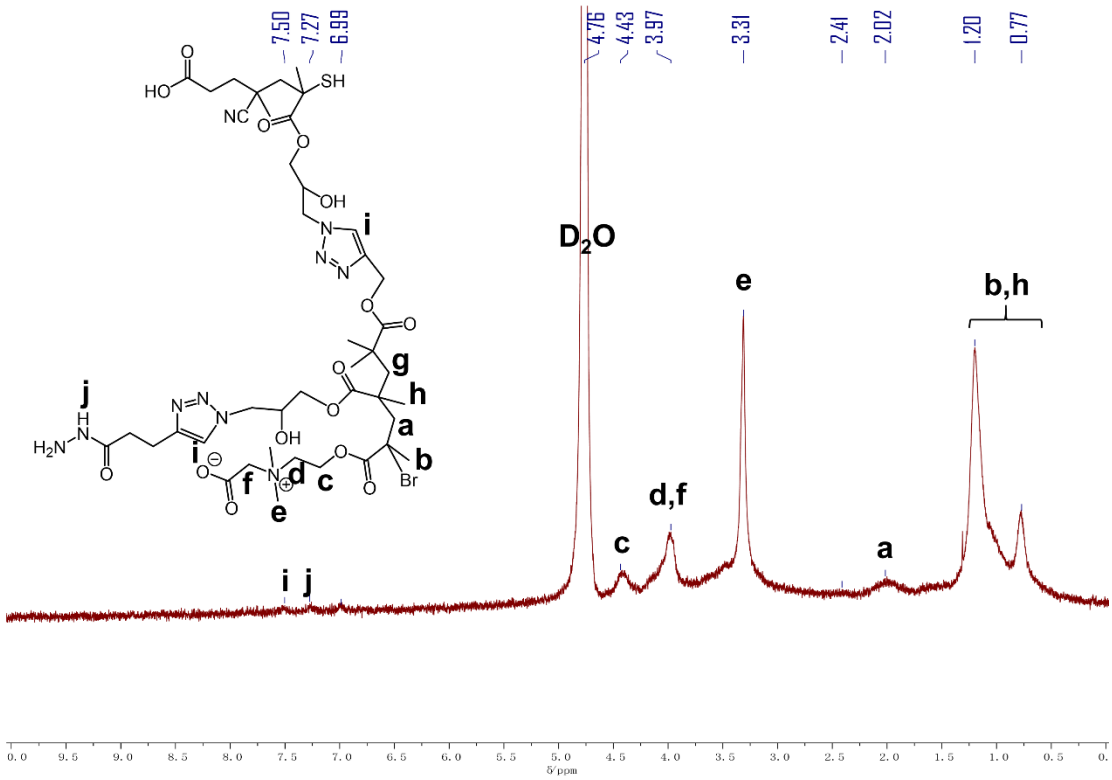

Supplementary Figure 14. ^{1}H NMR spectrum of BCPB in D_2O.

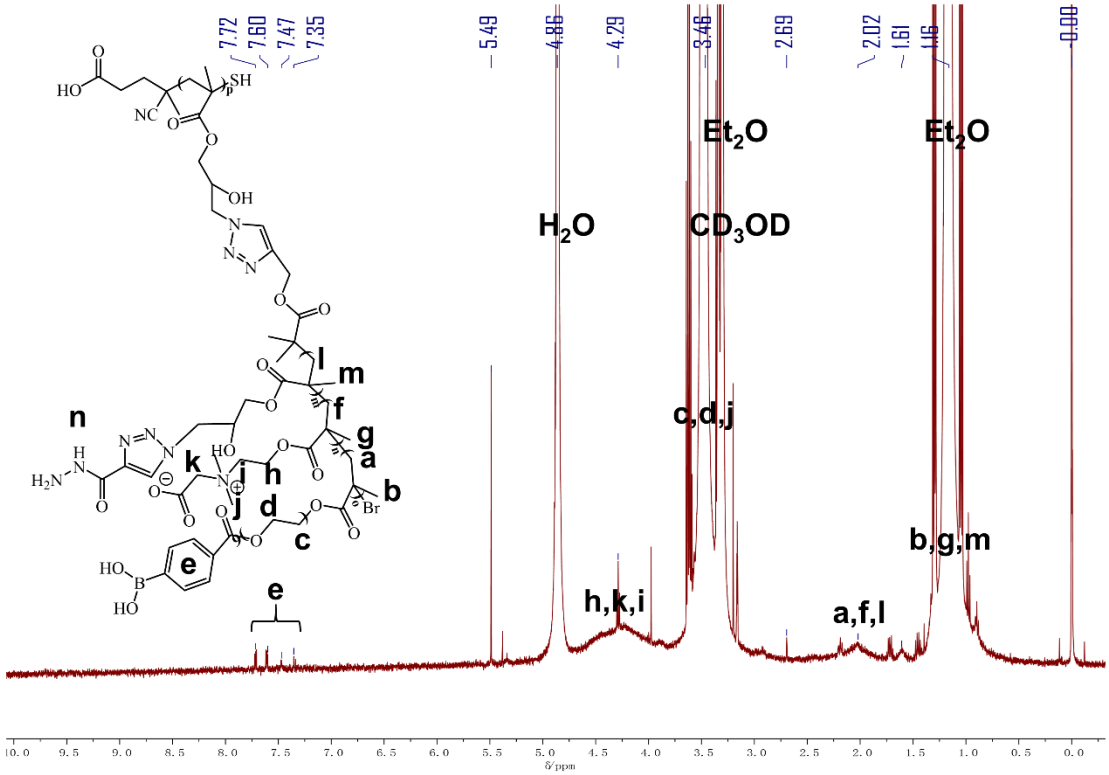

Supplementary Figure 15. ^{1}H NMR spectrum of BCPB-B in D_2O.

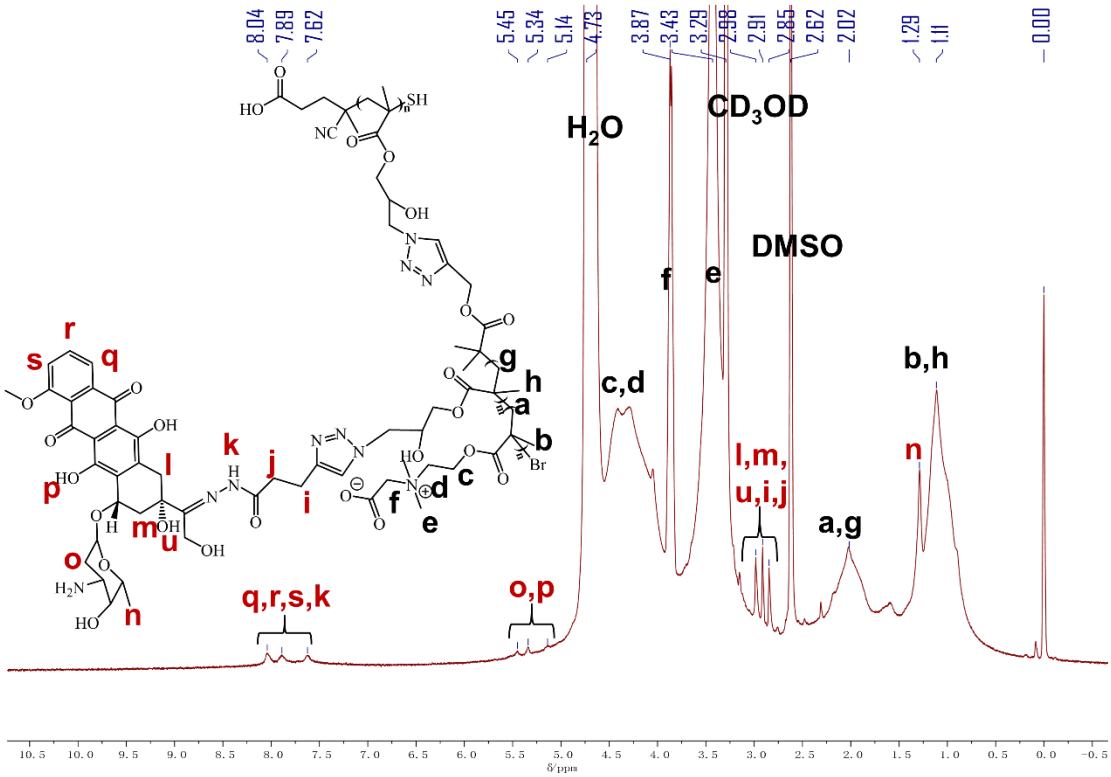

Supplementary Figure 16. ^{1}H NMR spectrum of BCPB-DOX in CD_3OD.

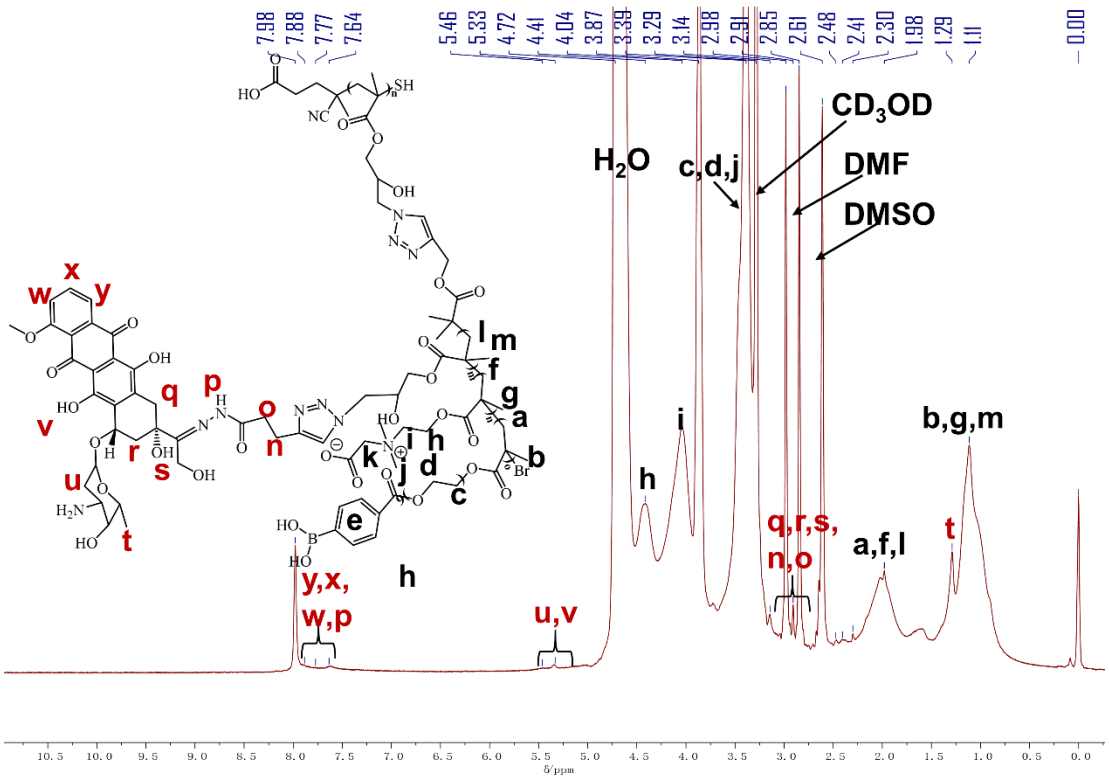

Supplementary Figure 17. ^{1}H NMR spectrum of BCPB-B-DOX in CD_3OD.

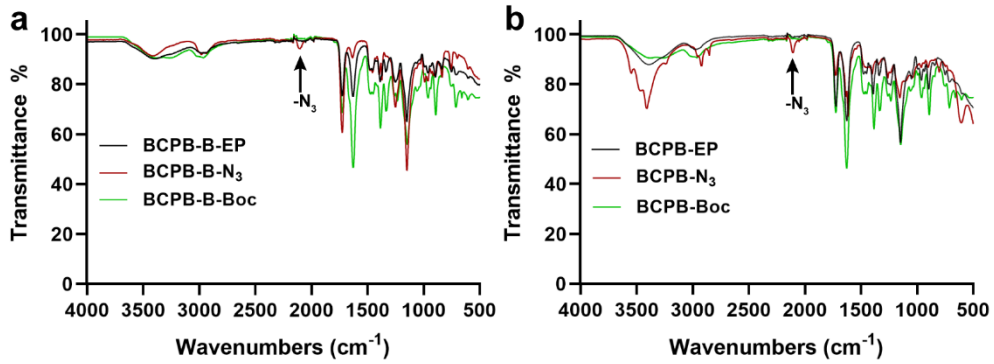

Supplementary Figure 18. a FTIR spectra of BCPB-B-EP, BCPB-B-N_3, and BCPB-B-Boc. **b** FTIR spectra of BCPB-EP, BCPB-N_3, and BCPB-Boc.

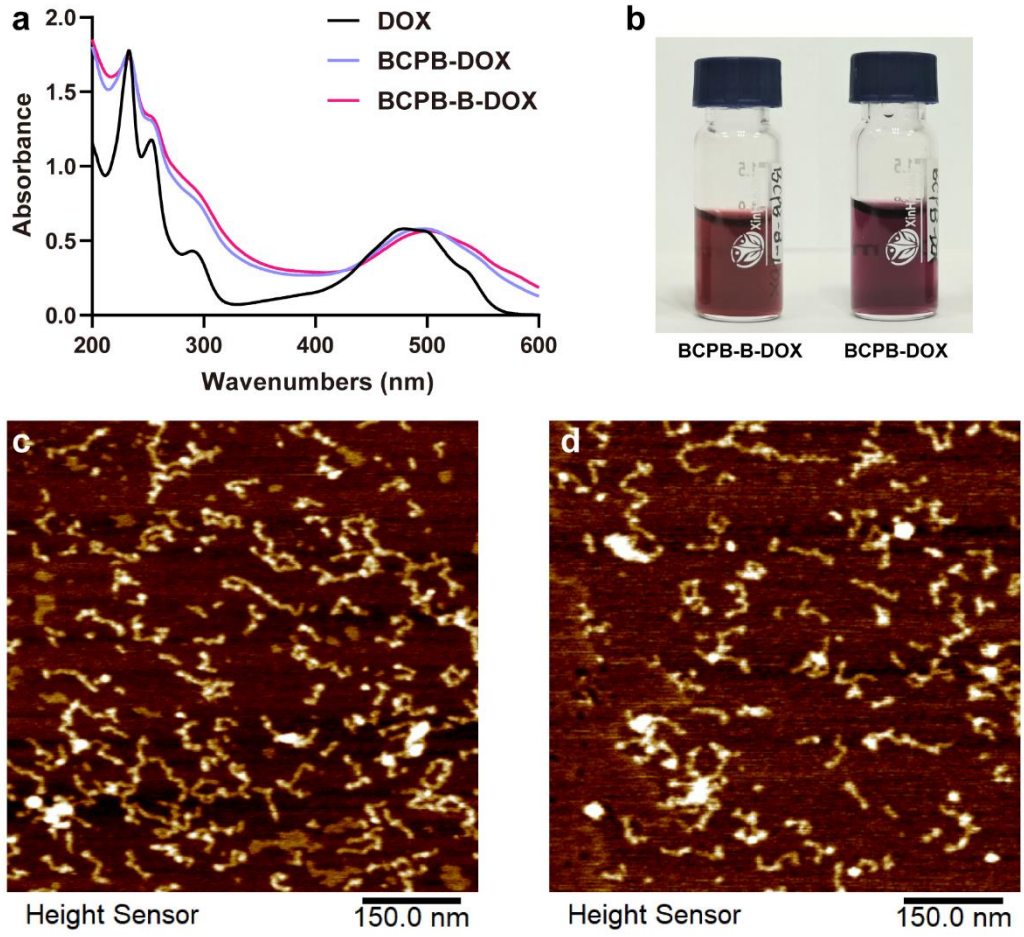

Supplementary Figure 19. a UV-vis spectra of free DOX, BPCB-DOX and BCPB-B-DOX. **b** Photographs of the water solutions of BCPB-B-DOX and BCPB-DOX at the concentrations normalized to 300 μg/mL DOX equivalent. **c**,**d** Typical AFM height images of BCPB-B-DOX (**c**) and BCBP-DOX (**d**) adsorbed on freshly cleaved mica from dilute water solutions. Scale bars = 150 nm.

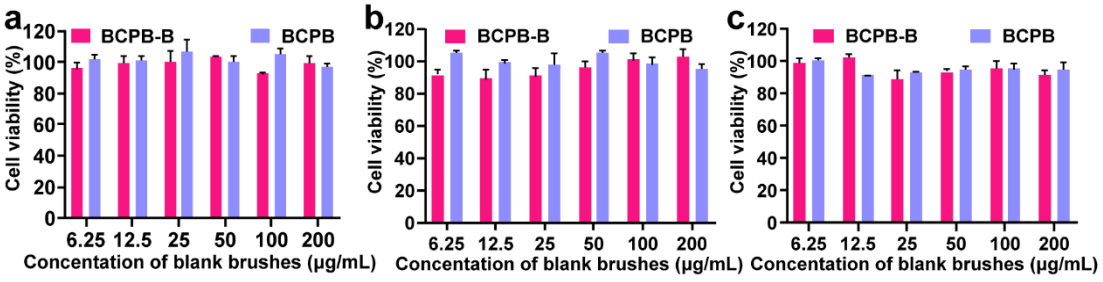

Supplementary Figure 20. Cytotoxicitiy of BCPB-B and BCPB against CT26 (**a**), MCF-7 (**b**), and HepG2 (**c**) cells determined by MTT assay after 24 h incubation.

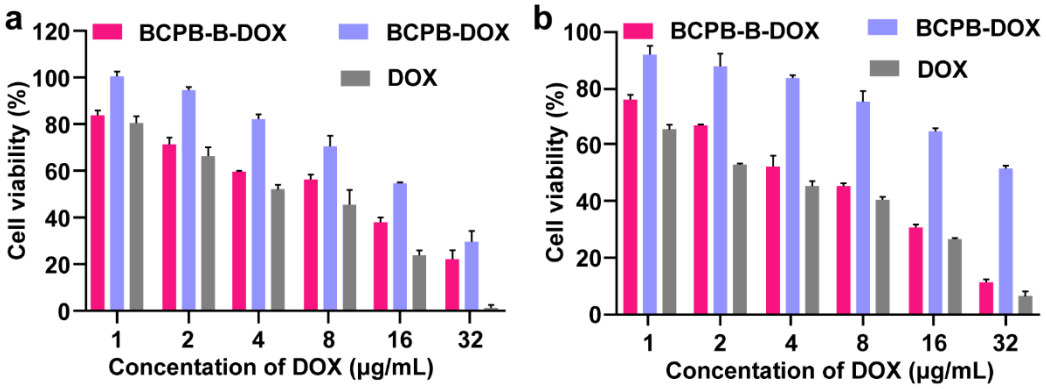

Supplementary Figure 21. Cytotoxicity of BCPB-B-DOX and BCPB-DOX against MCF-7 (**a**) and HepG2 (**b**) cells determined by MTT assay after 24 h incubation.

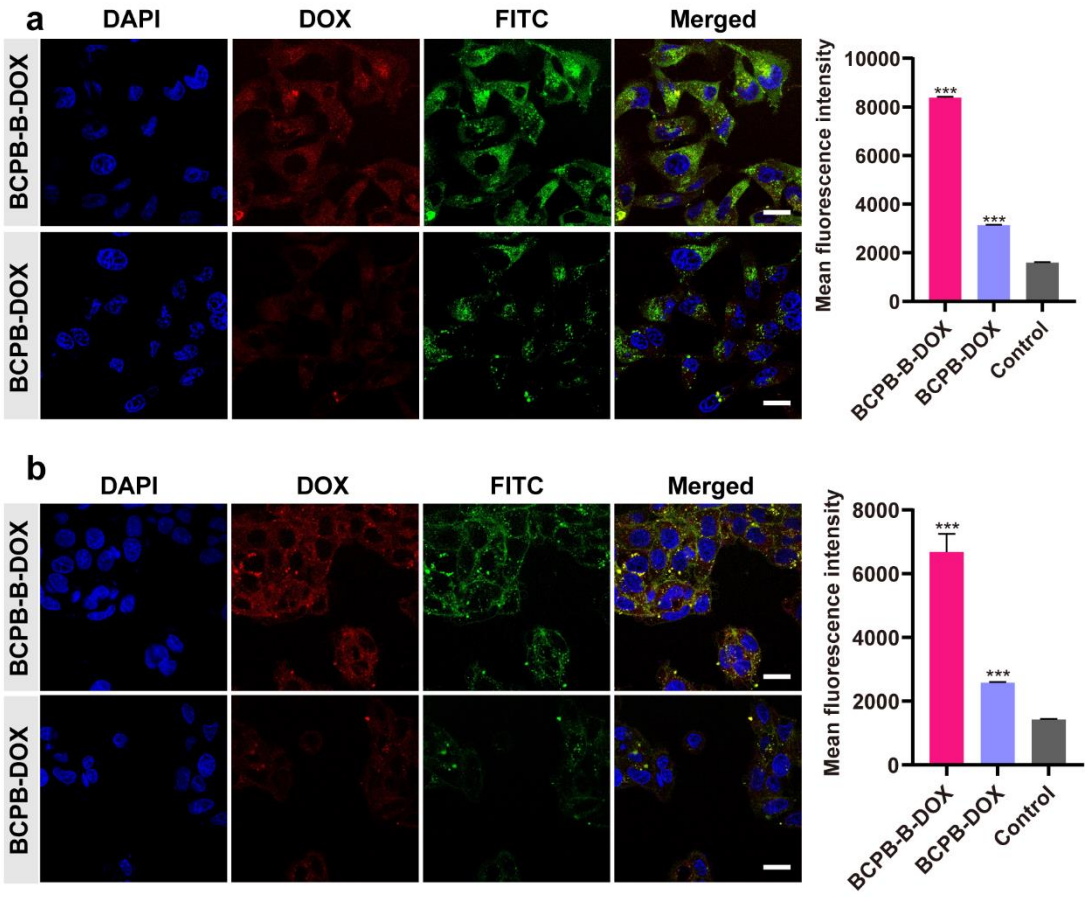

Supplementary Figure 22. a CLSM images and flow cytometry of MCF-7 cells after 2 h incubation with the FITC-labeled BCPB-B-DOX and BCPB-DOX, respectively. **b** CLSM images and flow cytometry of HepG2 cells after 2 h incubation with the FITC-labeled BCPB-B-DOX and BCPB-DOX, respectively. Scale bars = 20 μm. *P < 0.05, **P < 0.01, ***P < 0.001 compared with control.

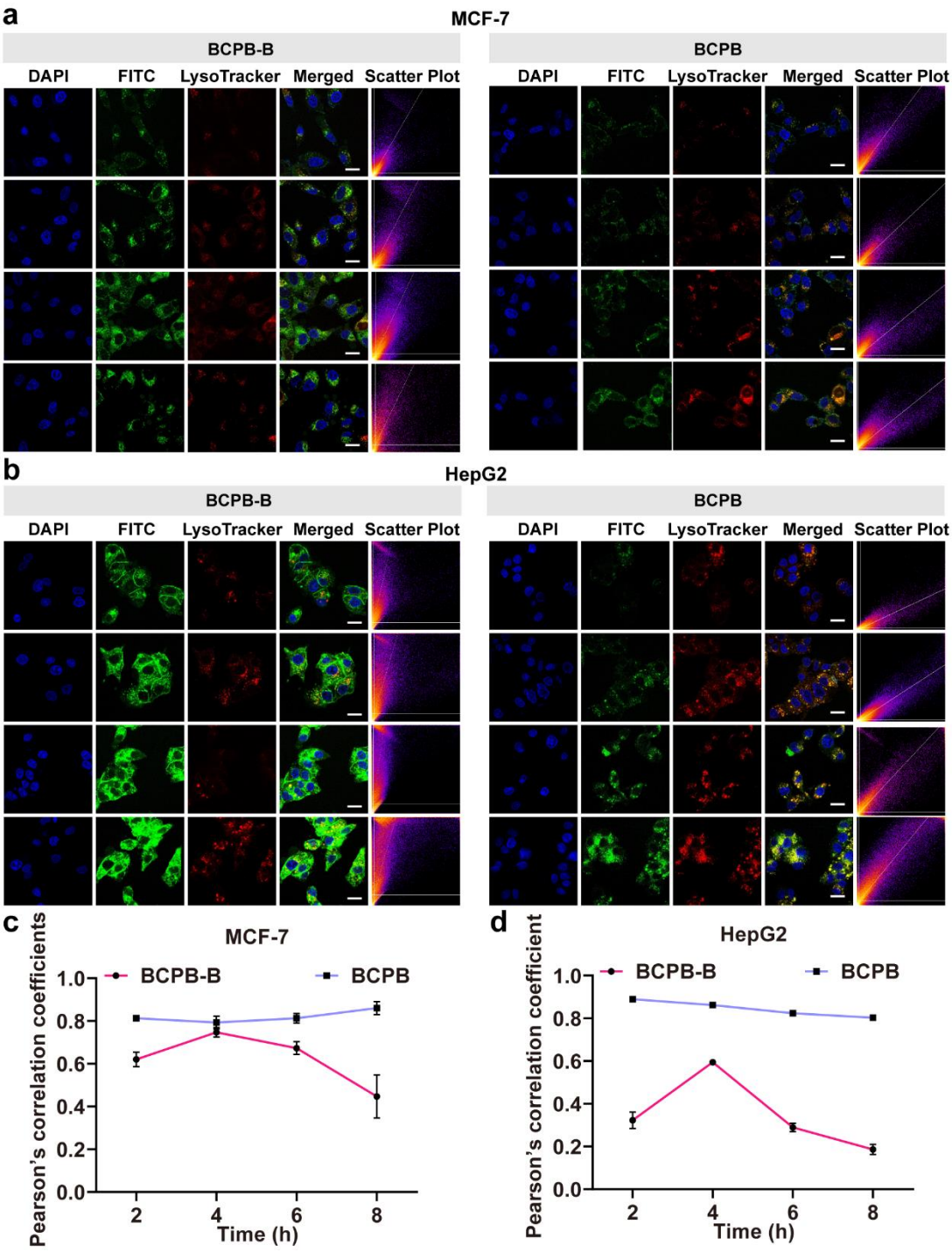

Supplementary Figure 23. a,**b** Colocalization observation by CLSM of FITC-labeled brushes (green) and LysoTracker (red) in MCF-7 cells (**a**) and HepG2 cells (**b**). Scale bars = 20 μm. **c**,**d** Evolution with time of the Pearson's correlation coefficients between the signals from the FITC-labeled CPBs and LysoTracker in MCF-7 cells (**c**) and HepG2 cells (**d**).

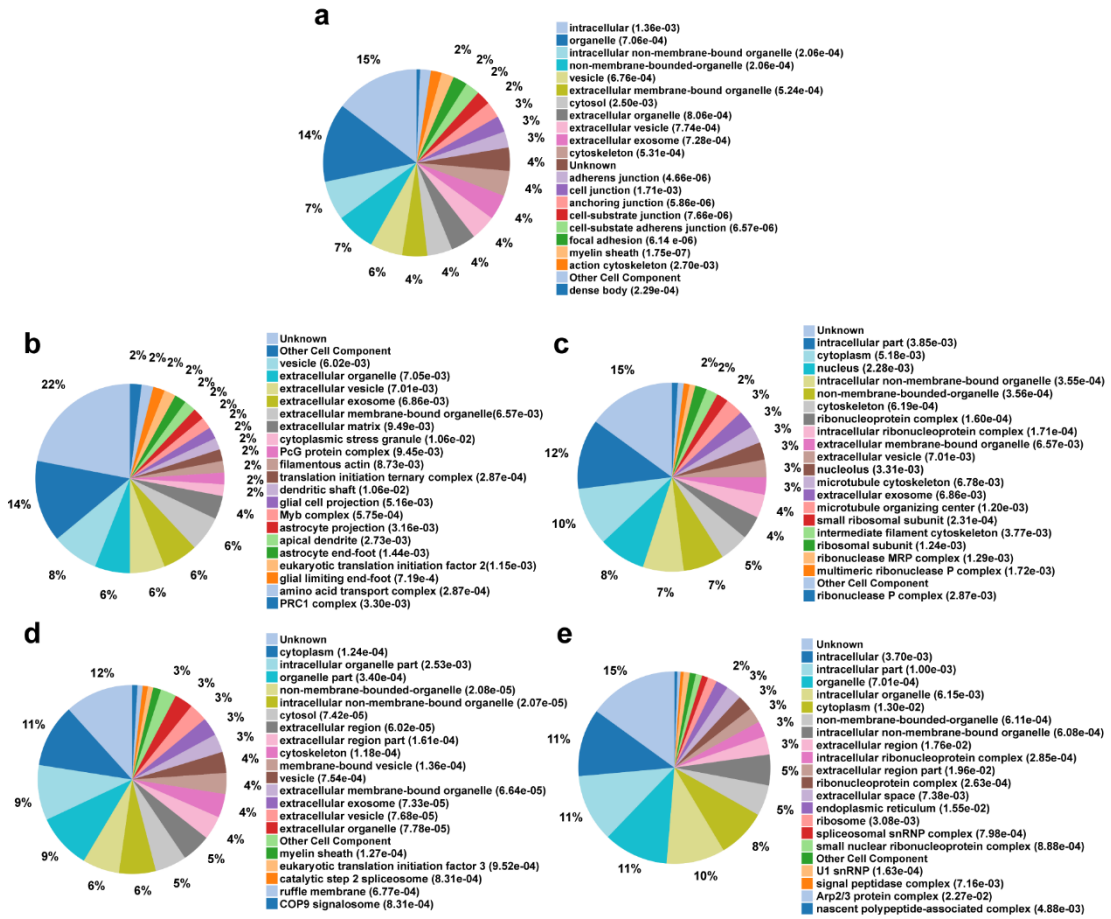

Supplementary Figure 24. GeneOntology (GO) pathway Cellular Component (CC) analysis: BCPB in CT26 cells (**a**), BCPB-B (**b**) and BCPB (**c**) in MCF-7 cells, BCPB-B (**d**) and BCPB (**e**) in HepG2 cells.

Table S1. Lysosomal membrane proteins adsorbed by BCPB-B and BCPB in tumor cells.

Cell line	Genes of BCPB-B group	Genes of BCPB group
CT26	Sec13; Ahnak; Flot1; HSP90AB	
MCF-7	SLC3A2	
HepG2	EEF1A1	

Table S2. Heat shock proteins adsorbed by BCPB-B and BCPB in the tumor cells.

Cell line	Genes of BCPB-B group	Genes of BCPB group
CT26	Hspa9, Hspa5, Hsp90b1, HSPH1, Hspd1, Hspa4l, Hspg2, HSP90AB1, HSPA8, HSPA4	Hpa9, Hpa5
MCF-7	HSPB1	
HepG2	HSPA5	

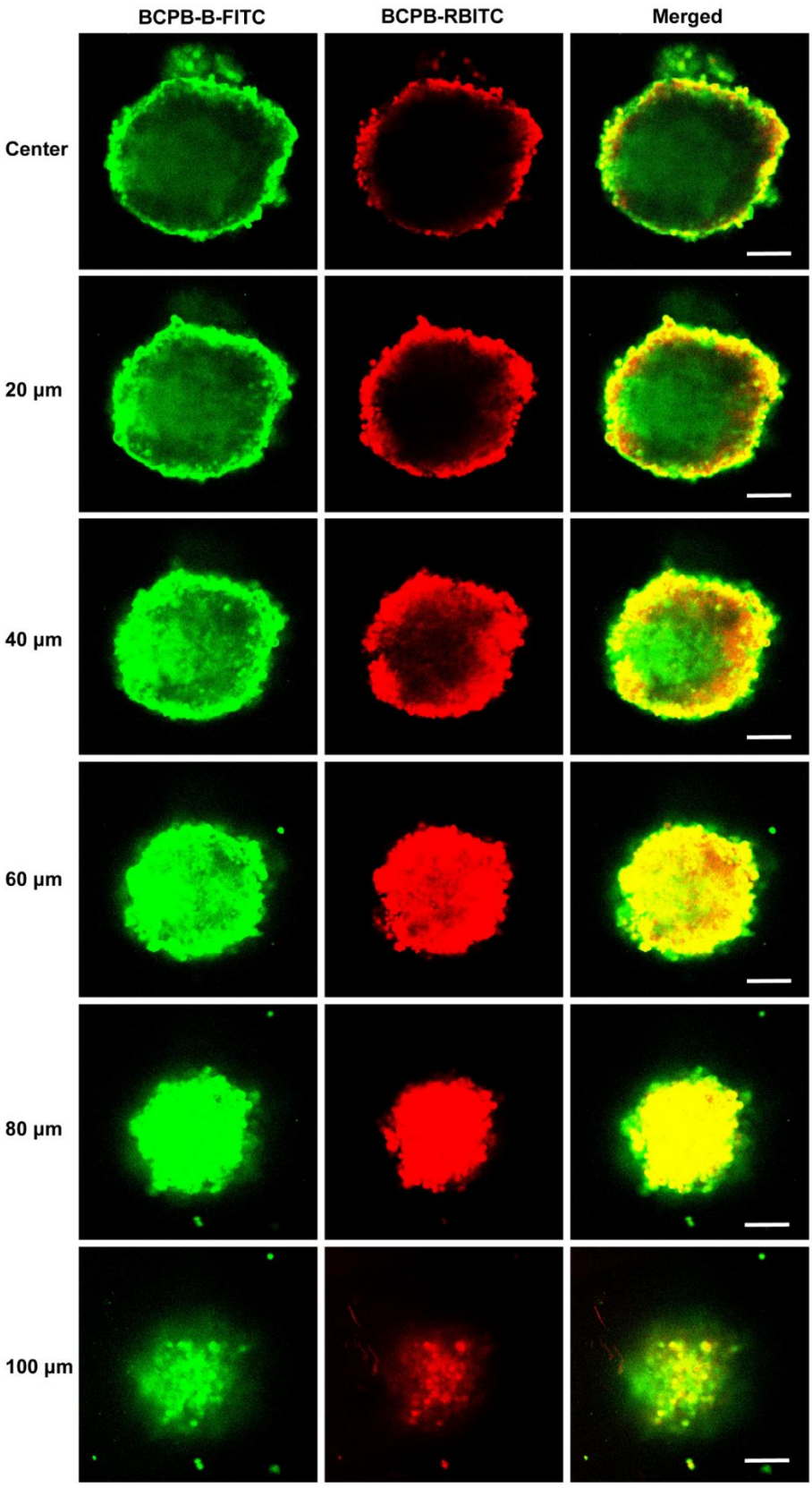

Supplementary Figure 25. Typical Z-stack images of the HepG2 MCs coincubated with the FITC-labeled BCPB-B and RBITC-labeled BCPB for 24 h acquired from the center to the top of the spheroid in a 20 μm interval. Scale bars = 100 μm.

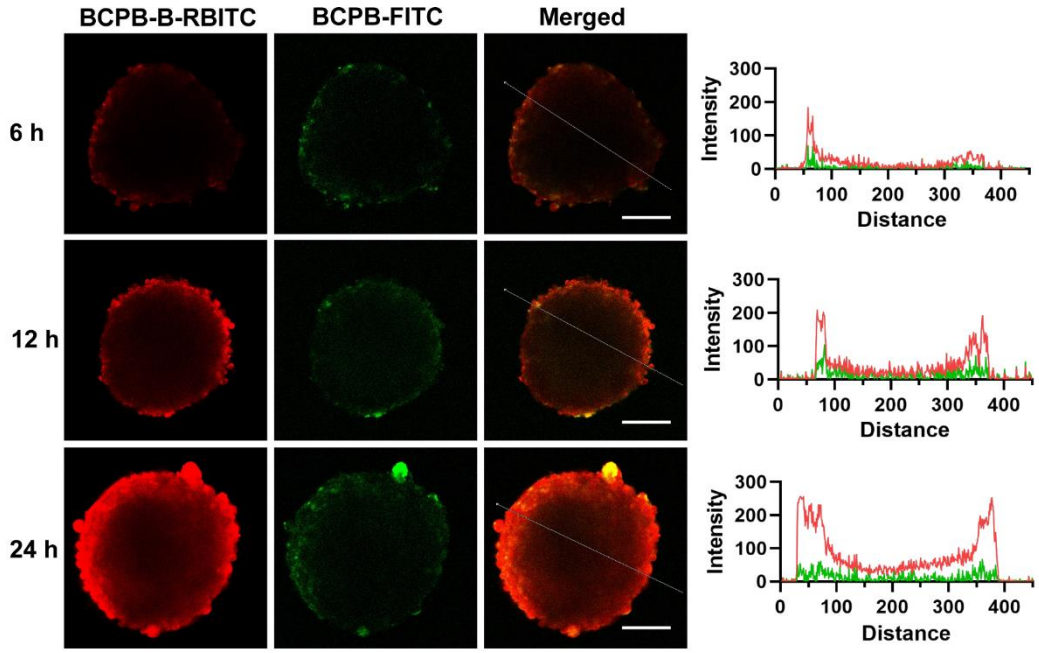

Supplementary Figure 26. CLSM images of the optical slices through the centers of the CT26 MCs coincubated with the RBITC-labeled BCPB-B and FITC-labeled BCPB for different periods (left). Scale bars = 100 μm. Fluorescence plate quantification data of the MCs (right).

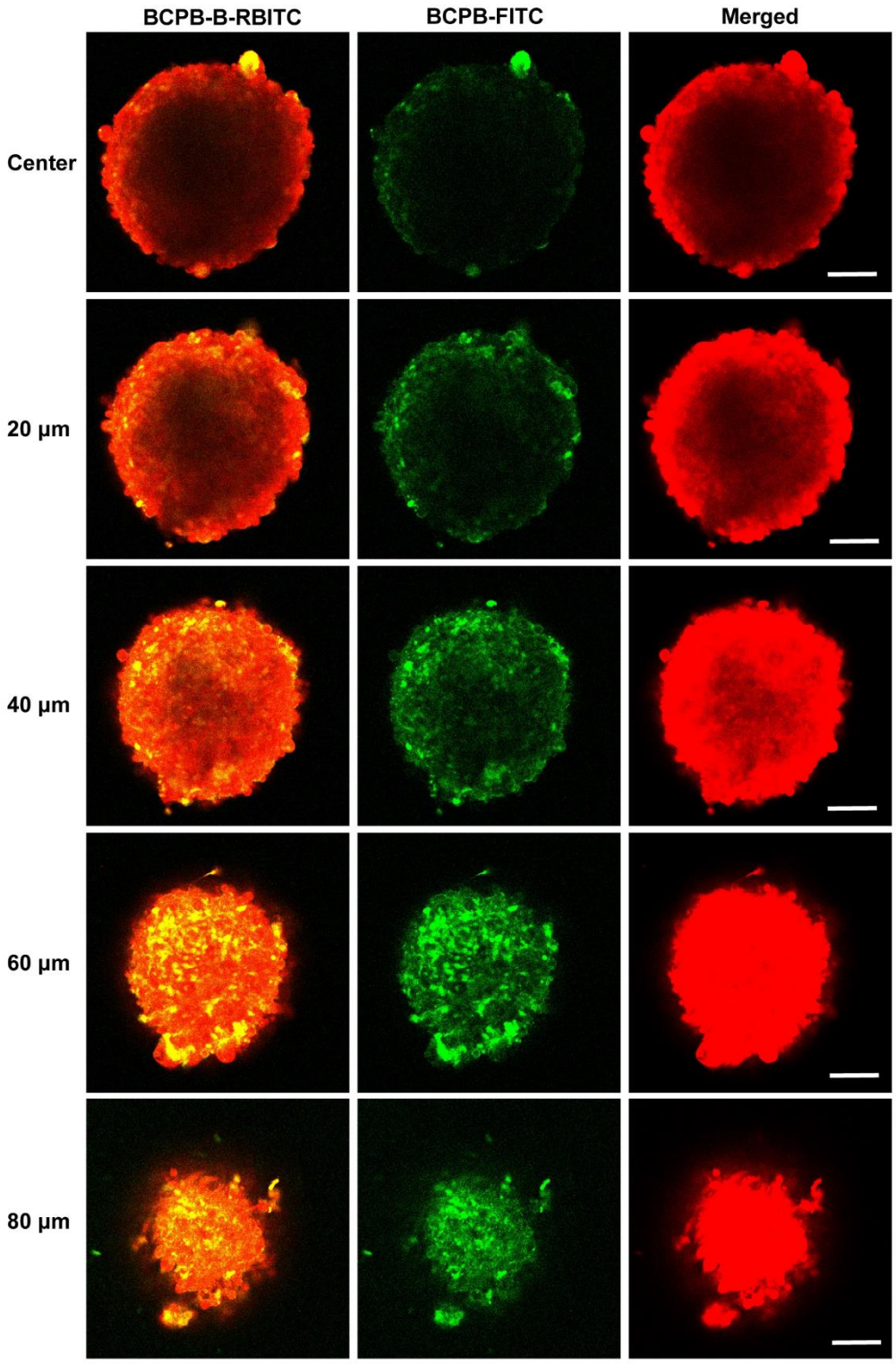

Supplementary Figure 27. Typical Z-stack images of the CT26 MCs coincubated with the RBITC-labeled BCPB-B and FITC-labeled BCPB for 24 h acquired from the center to the top of the spheroid in a 20 μm interval. Scale bars = 100 μm.

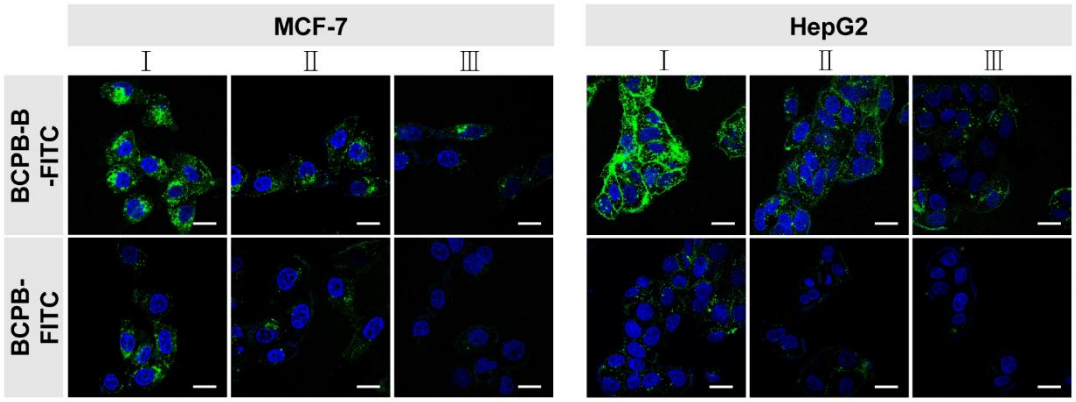

Supplementary Figure 28. Transcellular transfer study of the FITC-labeled BCPB-B and BCPB in MCF-7 and HepG2 cells. Scale bars = 20 μm.

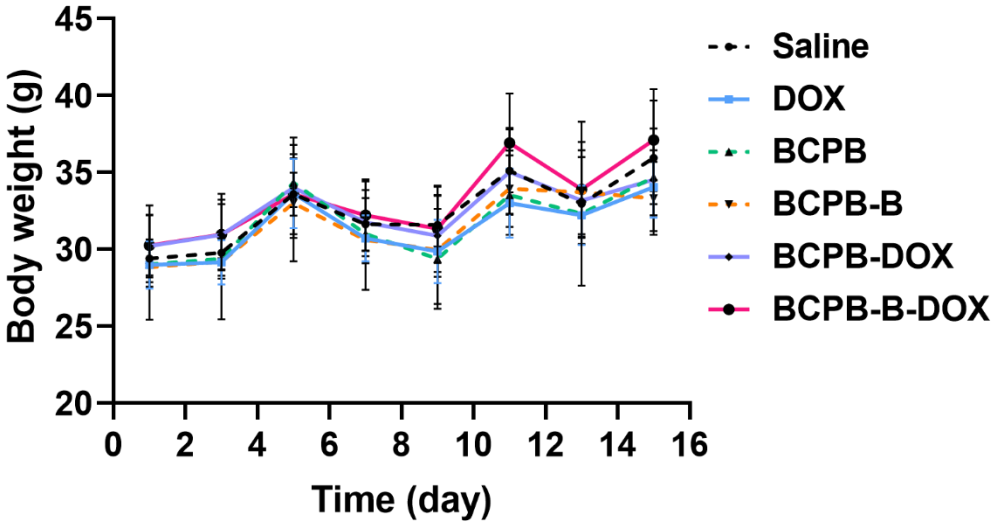

Supplementary Figure 29. Body weight change of the H22 tumor-bearing mice after one dose treatment with different protocols indicated.

References

1. Wang, X. *et al.* Doxorubicin delivery to 3D multicellular spheroids and tumors based on boronic acid-rich chitosan nanoparticles. *Biomaterials* **34**, 4667–4679 (2013).